JOURNAL OF AIRCRAFT
Vol. 41, No. 2, March–April 2004

Linkup Strength of 2024-T3 Bolted Lap Joint Panels with Multiple-Site Damage

Ala L. Hijazi,* Bert L. Smith,† and Thomas E. Lacy‡
Wichita State University, Wichita, Kansas 67260-0044

A modified linkup model has been developed for determining the residual strength of 2024-T3 aluminum panels with multiple-site damage. This model was developed by semi-empirical analysis of test data from flat unstiffened open-hole panels. The model was later validated with test data from 36 open-hole stiffened panels. During the investigation, 36 bolted lap joint panels with different crack configurations were tested to further validate the previously developed modified linkup model. Stress intensity factors for the modified linkup model for the different crack configurations were determined from finite element analysis with the FRANC2D/L code. The residual strengths predicted by the modified linkup model correlate well with the test data, as was the case with the earlier studies of the stiffened panels. The results for the bolted lap joint panels show a sudden reduction in the residual strength at the early stages of multiple-site damage followed by a gradual linear decrease with increasing multiple-site damage crack size. The results also demonstrate that a stress-intensity-factor-based solution can be formulated with empirical analysis of test data from a simple configuration and then used to analyze more complex configurations.

Nomenclature

a	=	lead crack half-length
a_n	=	nominal lead crack half-length
c	=	multiple-site damage (MSD) crack length
D	=	hole diameter
e	=	length of lead crack emerging from last hole, $a-(a_n+D/2)$
L	=	ligament length
ℓ	=	half-length of MSD crack and hole, $c+D/2$
K_I	=	mode I stress intensity factor
$K_{I(a)}$	=	lead crack stress intensity factor
$K_{I(\ell)}$	=	MSD crack stress intensity factor
β_a	=	geometric correction to stress intensity factor of lead crack
β_ℓ	=	geometric correction to stress intensity factor of the adjacent MSD crack
σ	=	remote stress (far-field applied stress)
σ_{LU}	=	residual strength based on Swift linkup model
σ_{test}	=	residual strength obtained from testing
σ_{WSU2}	=	residual strength based on WSU2 modified linkup model for 2024-T3
σ_{ys}	=	yield strength

Introduction

THE aging of aircraft fleets has increased the concern about aircraft structural integrity. As an aircraft is being used beyond its original design life, multiple-site damage (MSD) accumulates at critical locations, such as highly loaded fastener holes. The presence of MSD may reduce the ability of aircraft structure to carry the design load. An aircraft structure is often designed to maintain its structural integrity with relatively large (detectable) cracks. However, the presence of an array of small cracks, which may be below detectable limits, may reduce the residual strength of the structure below the required level. Thus, a methodology to evaluate the residual strength of aircraft skin with MSD is desirable.

A variety of approaches may be considered for evaluating the residual strength of panels with MSD. Net section yielding and linear elastic fracture mechanics (LEFM) are the most traditional approaches, and both have been found to give unreliable predictions for most structural and crack configurations for 2024-T3 aluminum alloy.[1] Thin, ductile fuselage skin material, such as 2024-T3 aluminum, typically exhibits large-scale crack tip yielding and significant amounts of stable crack extension before failure, which limits the applicability of LEFM-based techniques. Swift[2] introduced an analytical model to predict the residual strength of thin-sheet ductile materials with MSD cracks. This model is often referred to as the linkup model, or plastic-zone-touch model. The linkup model clearly shows an additional loss in strength from MSD; however, it does not accurately predict the magnitude of the loss for many geometric configurations.[3] This concern has prompted the development of modified models that maintain the simplicity of the linkup model yet give more accurate results.

The linkup model employs a combination of yielding and LEFM concepts. That is, it combines material yielding with the crack tip stress intensity factor (SIF). Because the linkup model is expressed in terms of the SIF, the assumption has been adopted that any modification or improvement of the model may be done with a semi-empirical analysis of test data from simplified geometric configurations. Then the modified model may be used for the analysis of any other (more complicated) geometric configurations, provided that the SIFs for the more complicated configurations can be determined. A semi-empirically modified linkup model has been developed by Smith et al.[3] for 2024-T3 aluminum alloy. This model was developed with test data from 40 unstiffened open-hole panels with MSD. The modified linkup model was later validated with test results from 36 different configurations of open-hole stiffened panels.[4] To further strengthen the assumption that the modified model could be developed with test data from simple configurations, then used to analyze more complicated configurations, it was validated against test data from 36 bolted lap joint panels with different crack configurations. This later validation based on bolted lap joints is presented in this paper. Out of the 36 panels, 9 panels had a lead crack only (no MSD cracks at the adjacent holes), whereas each of the remaining 27 had a lead crack as well as MSD cracks at the adjacent holes along the crack line. A comparison of the residual strengths obtained from testing with the residual strengths predicted by the

Received 13 June 2002; revision received 15 May 2003; accepted for publication 20 June 2003.

*Postdoctoral Research Fellow, Department of Aerospace Engineering, 1845 Fairmount.

†Professor, Department of Aerospace Engineering, 1845 Fairmount. Senior Member AIAA.

‡Assistant Professor, Department of Aerospace Engineering, 1845 Fairmount. Member AIAA.

modified linkup model showed that the accuracy of the model was retained.

The residual strength is defined herein as the remote stress at which failure of the ligament between the lead crack tip and the adjacent MSD crack tip occurs. In the case of the panels with a lead crack but no MSD cracks, the residual strength is the remote stress at which failure of the ligament between the lead crack tip and the adjacent fastener hole occurs.

Linkup Model

The linkup model is based on the assumption that the ligament L, shown in Fig. 1, between the lead crack tip and the adjacent MSD crack tip, will fail from plastic collapse when the plastic zone at the tip of the lead crack touches the plastic zone at the tip of the adjacent MSD crack. Although the schematic diagram shown in Fig. 1 is a flat unstiffened open-hole panel, the linkup model is formulated so that it may be used with more complex configurations, as long as the SIFs of the lead crack tip and the adjacent MSD crack tip can be determined. According to the linkup model, the residual strength, the value of remote stress at which linkup (ligament failure) occurs, is given as follows[2]:

$$\sigma_{\mathrm{LU}} = \sigma_{\mathrm{ys}} \sqrt{\frac{2L}{a\beta_a^2 + \ell\beta_\ell^2}} \tag{1}$$

Several modifications of the linkup model have been developed and reported in the literature.[5,6] Smith et al.[3] developed two empirically modified linkup models based on the semi-empirical analysis of 40 different configurations of flat unstiffened open-hole panels that included three different panel widths, two different panel thicknesses, two different grain directions, both bare and clad material, and a variety of different lead crack lengths and ligament lengths.

These two models were further validated against test data from 36 different configurations of stiffened panels.[4] Of these panels, 21 were single-bay stiffened panels with the lead crack centered between stiffeners, whereas the other 15 were two-bay stiffened panels with the lead crack centered under a severed center stiffener. These models were developed for use with standard MIL-HDBK-5G[7] A-basis and B-basis yield strength values.

Although two modified linkup models were developed by Smith et al.,[3,4] only the more accurate of the two will be included herein. This model, given in Eq. (2), was referred to in Refs. 3 and 4 as the WSU2 model, and this same nomenclature will be used herein. This model is expressed in terms of the Swift[2] linkup stress given in Eq. (1), the ligament length L, and the two constants C_1 and C_2. The WSU2 model gives the residual strength as follows:

$$\sigma_{\mathrm{WSU2}} = \frac{\sigma_{\mathrm{LU}}}{C_1\,\ell n(L) + C_2 + 1} \tag{2}$$

The constants C_1 and C_2 are the regression coefficients determined from the semi-empirical analysis based on the test data from the 40 unstiffened open-hole panels.[3] Normalizing the Swift[2] linkup stress σ_{LU} by the factor $[C_1\,\ell n(L) + C_2 + 1]$ results in improved estimates of residual strength.[3,4] The values of the coefficients are $C_1 = 0.3065$ and $C_2 = 0.3123$ when A-basis yield strengths are used and $C_1 = 0.3054$ and $C_2 = 0.3502$ when B-basis yield strengths are used.

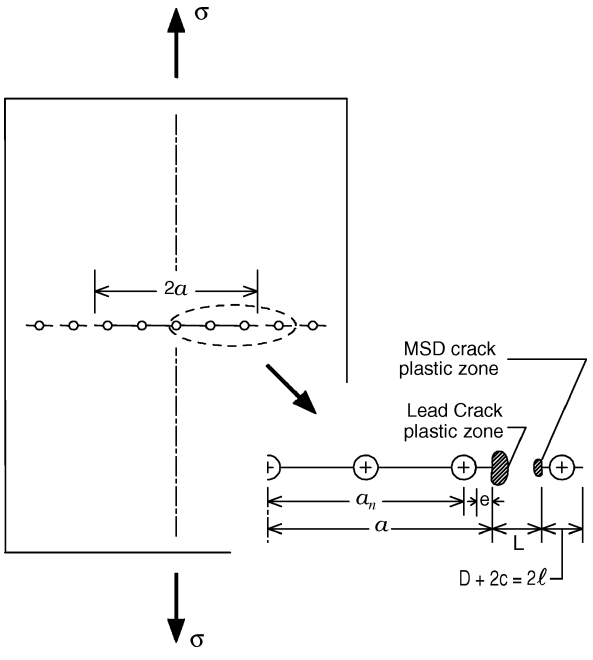

Fig. 1 Schematic diagram of a panel with MSD.

Experimental Setup and Test Data

The test matrix included 36 panels, each with different crack configuration. Details of the crack configurations for the 36 panels are given in Table 1. A servohydraulic testing machine was used to generate the load required to produce ligament failure. The tests were conducted under stroke control (to avoid total failure of the test panel after the first linkup) at a rate of 0.01 in./min. Tests were terminated immediately after the first ligament failure (linkup) occurred. The ligament L (Fig. 1) was monitored with a closed-circuit monitoring system that consisted of a video camera with a high magnification lens linked to a monitor and a video cassette recorder.

Each bolted lap joint test panel (Fig. 2) was 24 in. wide and was constructed with 0.056-in.-thick clad 2024-T3 aluminum. The load was applied perpendicular to the grain direction. The A-basis and B-basis yield strength values for the material are 39 and 40 ksi, respectively.[7] The two sheets of the joint were overlapped 3 in. and were fastened together with three rows of 0.1875-in.-diam steel bolts. The holes were also 0.1875 in. in diameter in an attempt to provide a neat fit with no interference, and the nuts were lightly

Table 1 Panels crack configurations

Panel	$2a_n$, in.	a, in.	e, in.	c, in.	ℓ, in.	L, in.
1	8	4.19375	0.10	0	——	0.7125
2	8	4.19375	0.10	0.05	0.14375	0.6625
3	8	4.19375	0.10	0.10	0.19375	0.6125
4	8	4.24375	0.15	0	——	0.6625
5	8	4.24375	0.15	0.05	0.14375	0.6125
6	8	4.24375	0.15	0.10	0.19375	0.5625
7	8	4.24375	0.15	0.15	0.24375	0.5125
8	8	4.29375	0.20	0	——	0.6125
9	8	4.29375	0.20	0.05	0.14375	0.5625
10	8	4.29375	0.20	0.10	0.19375	0.5125
11	8	4.29375	0.20	0.15	0.24375	0.4625
12	8	4.29375	0.20	0.20	0.29375	0.4125
13	10	5.19375	0.10	0	——	0.7125
14	10	5.19375	0.10	0.05	0.14375	0.6625
15	10	5.19375	0.10	0.10	0.19375	0.6125
16	10	5.24375	0.15	0	——	0.6625
17	10	5.24375	0.15	0.05	0.14375	0.6125
18	10	5.24375	0.15	0.10	0.19375	0.5625
19	10	5.24375	0.15	0.15	0.24375	0.5125
20	10	5.29375	0.20	0	——	0.6125
21	10	5.29375	0.20	0.05	0.14375	0.5625
22	10	5.29375	0.20	0.10	0.19375	0.5125
23	10	5.29375	0.20	0.15	0.24375	0.4625
24	10	5.29375	0.20	0.20	0.29375	0.4125
25	12	6.19375	0.10	0	——	0.7125
26	12	6.19375	0.10	0.05	0.14375	0.6625
27	12	6.19375	0.10	0.10	0.19375	0.6125
28	12	6.24375	0.15	0	——	0.6625
29	12	6.24375	0.15	0.05	0.14375	0.6125
30	12	6.24375	0.15	0.10	0.19375	0.5625
31	12	6.24375	0.15	0.15	0.24375	0.5125
32	12	6.29375	0.20	0	——	0.6125
33	12	6.29375	0.20	0.05	0.14375	0.5625
34	12	6.29375	0.20	0.10	0.19375	0.5125
35	12	6.29375	0.20	0.15	0.24375	0.4625
36	12	6.29375	0.20	0.20	0.29375	0.4125

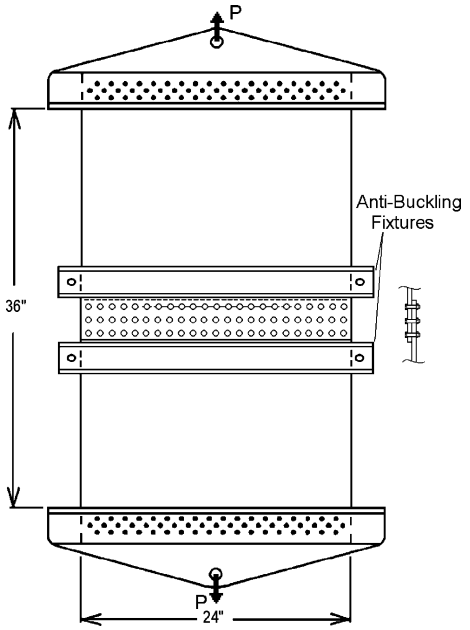

Fig. 2 Schematic of a bolted lap joint test panel.

torqued. The bolt pitch, row spacing, and edge distance were 1, 1, and 0.5 in., respectively. An antibuckling fixture consisting of a C channel on each side of the panel was placed next to the overlap, as shown in Fig. 2, to prevent out-of-plane movement. Because the modified linkup model was developed from test data for panels with antibuckling fixtures, the model is only reliable for panels with negligible out-of-plane displacement along the row with MSD. The lead crack was centered in the middle of the panel. The MSD cracks were introduced at the fastener holes adjacent to the lead crack tips. The cracks were produced with a jewelers saw and were 0.007 in. thick. Earlier research[3] showed that cracks produced by saw cut gave the same results as 0.005-in.-diam cracks produced by an electrodischarge machine (EDM), although the EDM cracks gave more consistent results. There is a concern as to whether crack tips produced by EDM or saw cut may be used to produce reliable results for residual strength tests, as compared with results produced from fatigue cracked specimens. Dawicke et al.[8] demonstrated a significant difference in the results between using these two types of cracks. On the other hand, Heinimann[9] and Secton[10] concluded that EDM slots provided a suitable comparative method for residual strength tests requiring consistent initial configurations.

The lead crack and the MSD cracks were cut across the upper row of fasteners because this is the most critical row with the largest fastener loads and the largest bypass stress. Figure 2 shows an actual bolted lap joint panel, whereas Fig. 1 is a schematic diagram of a panel, which more clearly illustrates the lead crack and the MSD cracks at the adjacent holes.

Geometric Corrections to Stress Intensity Factor

Determining the effects of geometry on the crack tip SIF is essential for using any SIF-based model, such as the linkup model. Classical solutions for the geometric corrections (beta or β) to stress intensity factors are available for a limited number of configurations in the literature. Finite element analysis may also be used to determine the betas for a particular structural configuration. The idea of using finite element analysis for determining the betas is quite simple. As an example, to determine the stiffener effect for a stiffened panel, which we shall call β_s, a finite element solution may be used to determine the SIFs of both the stiffened panel and the unstiffened panel. Then the value of β_s is determined as the ratio of the SIF for the stiffened panel to that of the unstiffened panel, both with the same crack configuration. This simple comparative technique can be used to determine any geometric effect on the crack tip SIF. For the bolted lap joint panels, where there were no available classical solutions for determining the betas, finite element analysis was used. The fracture analysis code for layered structures (FRANC2D/L)[11] was used for modeling and analyzing the different crack configurations that were tested to determine the SIFs. Then the betas were determined from the SIF values.

The determination of SIFs for cracks at fastener holes in mechanically fastened joints is a central issue in damage tolerance analysis. Finite element analysis is often used because of the structural complexity along with variations in fastener load transfer and fastener interference. The modeling of the fasteners is a critical factor in mechanically fastened lap joint analysis. Explicit representation of the fasteners (where the fastener hole, shank, and interference are being modeled) is one option for obtaining accurate solutions. Given the considerable number of fasteners in a typical aircraft structural joint, explicit representation of all fasteners becomes impractical because of the huge number of degrees of freedom associated with such an analysis. Cope and Lacy[12] used a combination of explicit and spring element representations of fasteners to model single shear lap joints. The fasteners in the row along the crack line were modeled explicitly, and spring element representation was used for modeling the fasteners in the other rows. Their approach was effective in reducing the required number of degrees of freedom, and it provided good estimates of load transfer and relative displacement between mating sheets.

The 36 crack configurations of the bolted lap joint panel were modeled and analyzed. Because of symmetry, only one-half of the test panel was modeled. Plane stress T-6 (Ref. 11) elements were used. A refined mesh was used in the areas of explicitly modeled fasteners, and a coarser mesh was used elsewhere. Symmetry boundary conditions were applied to the centerline edge. Equally distributed loads were applied to the top and bottom edges of the model. Fixity conditions were applied to one node at the midlength to prevent rigid-body motion. The two sheets were modeled in separate layers, then they were joined together with three rows of fasteners. The fasteners in the top row (along the crack line) were modeled explicitly in both layers with nonlinear interface[11] elements at the interface between fastener and sheet and adhesive[11] elements between the overlapping fastener elements in both sheets to provide distributed shear load transfer.[12] Linear properties were used for the interface elements to produce bearing stress on one side of the fastener hole and gap on the other side. The other two rows of fasteners were modeled with rivet (spring) elements between coincident nodes in both sheets. Figure 3 shows a portion of the finite element mesh, where the explicitly modeled fasteners and crack tips can be seen. The shear modulus G_F of the fastener adhesive elements was determined by equating the fastener deflection based on a strain energy relation to a Swift[13] empirical relation and then solving for

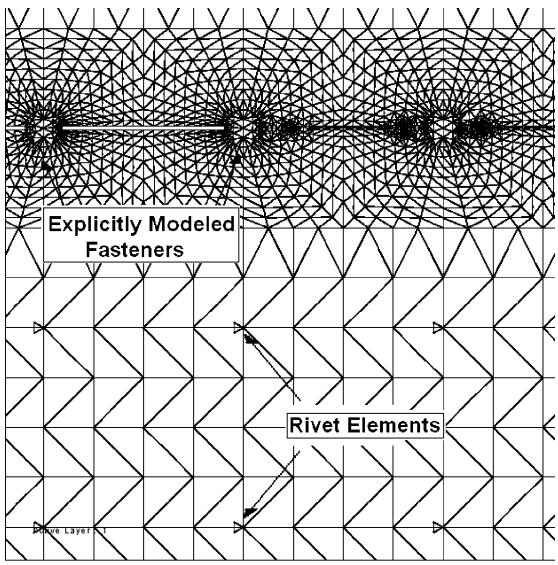

Fig. 3 Portion of the FRANC2D/L finite element mesh for bolted lap joint panel.

Table 2 Total geometric effect corrections to SIF for the panels

Panel	β_a	β_ℓ
1	0.913	——
2	0.922	2.506
3	0.935	2.323
4	0.894	——
5	0.904	2.574
6	0.918	2.393
7	0.934	2.268
8	0.881	——
9	0.889	2.656
10	0.905	2.466
11	0.923	2.346
12	0.944	2.294
13	0.939	——
14	0.948	2.853
15	0.961	2.642
16	0.921	——
17	0.93	2.93
18	0.941	2.72
19	0.958	2.572
20	0.905	——
21	0.915	3.034
22	0.93	2.799
23	0.949	2.663
24	0.971	2.613
25	0.983	——
26	0.992	3.314
27	1.007	3.028
28	0.968	——
29	0.979	3.403
30	0.994	3.113
31	1.012	2.952
32	0.953	——
33	0.964	3.503
34	0.981	3.218
35	1.001	3.059
36	1.025	2.988

the shear modulus.[12] This formulation accounted for both the fastener and the sheet material properties and combined both shearing and bending stiffness to determine the shear modulus for adhesive elements and the shear stiffness for the spring elements.[1] A linear-dynamic relaxation[11] analysis was performed to obtain the stress intensity factors for the lead crack $K_{I(a)}$ and the adjacent tip of the MSD crack $K_{I(\ell)}$. The beta for the lead crack tip, β_a, and the beta for the MSD crack tip, β_ℓ, for each crack configuration were each determined by dividing the SIF obtained from the analysis by the SIF for an equivalent length crack in an infinite domain as follows:

$$\beta_a = K_{I(a)} \Big/ \sigma\sqrt{\pi a} \tag{3}$$

$$\beta_\ell = K_{I(\ell)} \Big/ \sigma\sqrt{\pi \ell} \tag{4}$$

Table 2 contains the resulting beta values for each of the 36 configurations. Because 9 of the 36 configurations did not have MSD cracks, there were no β_ℓ values for those configurations.

Results

The residual strengths (remote stresses causing ligament failure) for the 36 panels obtained from testing along with the residual strengths predicted by the linkup model [Eq. (1)] and the modified linkup model [Eq. (2)] are given in Tables 3 and 4. Table 3 has the residual strengths predicted by the linkup (LU) and the modified LU (WSU2) models when the A-basis yield strength value is used, and Table 4 has the predicted residual strengths when the B-basis yield strength is used. The errors produced by each of the two models are also given in Tables 3 and 4. Error is defined here as the absolute value of the percent difference between test value and analytical model prediction. There were 9 of the 36 configurations with no MSD cracks. For these nine panels, the residual strength was calculated by letting $\beta_\ell = 0$ in Eqs. (1) and (2). With the A-basis yield strengths, the average error for the residual strength predictions of the LU model [Eq. (1)] was 18.68%, whereas the average error for the modified LU model, WSU2, [Eq. (2)] was 4.7%. When using B-basis yield strengths, the average error was 21.72% for the LU model and 4.14% for the modified LU model. These errors show that the modified LU model is significantly more accurate than the original Swift LU model. Figure 4 shows these same results graphically, where it gives the residual strengths from the LU model and the modified LU model vs the test values. In both cases,

Table 3 Residual strengths based on A basis yield strengths

Panel	σ_{test}, ksi	σ_{LU}, ksi	σ_{WSU2}, ksi	σ_{LU}, % error	σ_{WSU2}, % error
1	20.91	24.89	20.6	19.07	1.47
2	18.38	21.24	17.91	15.58	2.55
3	16.79	19.89	17.12	18.52	1.99
4	20.02	24.36	20.54	21.68	2.59
5	18.38	20.52	17.66	11.68	3.9
6	16.44	19.11	16.83	16.25	2.34
7	15.45	17.74	16.02	14.8	3.66
8	19.85	23.66	20.36	19.2	2.58
9	17.38	19.7	17.35	13.39	0.18
10	16.47	18.22	16.45	10.62	0.11
11	15.34	16.78	15.59	9.39	1.67
12	14.72	15.28	14.68	3.8	0.28
13	17.27	21.76	18	25.97	4.25
14	15.56	18.58	15.66	19.38	0.65
15	14.88	17.4	14.98	16.95	0.64
16	17.17	21.29	17.95	23.99	4.54
17	15.36	17.97	15.46	16.93	0.62
18	14.11	16.78	14.77	18.91	4.68
19	13.1	15.58	14.07	18.96	7.42
20	16.71	20.73	17.84	24.09	6.78
21	14.82	17.25	15.18	16.39	2.46
22	13.96	15.99	14.44	14.55	3.44
23	12.8	14.72	13.68	15.02	6.9
24	11.88	13.39	12.87	12.74	8.31
25	14.97	19.04	15.75	27.19	5.25
26	12.95	16.2	13.66	25.08	5.46
27	12.51	15.2	13.08	21.49	4.55
28	14.78	18.55	15.64	25.55	5.85
29	12.74	15.61	13.43	22.54	5.46
30	11.79	14.58	12.84	23.71	8.91
31	10.88	13.53	12.21	24.37	12.31
32	14.24	18.05	15.54	26.77	9.09
33	12.25	14.99	13.2	22.43	7.78
34	11.57	13.91	12.56	20.16	8.51
35	10.75	12.8	11.9	19.05	10.65
36	10.04	11.66	11.2	16.12	11.56
Average				18.68	4.7

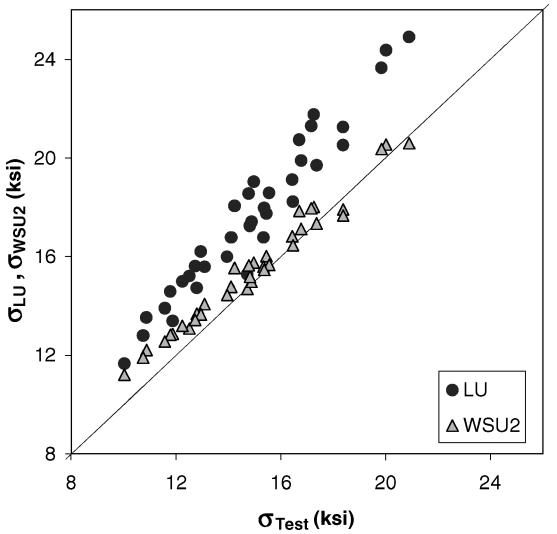

Fig. 4 Test results compared with LU and WSU2 models predictions (A basis).

Table 4 Residual strengths based on B-basis yield strengths

Panel	σ_{test}, ksi	σ_{LU}, ksi	σ_{WSU2}, ksi	σ_{LU}, % error	σ_{WSU2}, % error
1	20.91	25.53	20.48	22.12	2.04
2	18.38	21.79	17.79	18.55	3.18
3	16.79	20.40	17.00	21.56	1.26
4	20.02	24.99	20.41	24.80	1.93
5	18.38	21.05	17.53	14.54	4.59
6	16.44	19.60	16.69	19.23	1.52
7	15.45	18.19	15.87	17.74	2.73
8	19.85	24.26	20.21	22.26	1.84
9	17.38	20.21	17.21	16.30	0.98
10	16.47	18.69	16.31	13.45	1.01
11	15.34	17.21	15.44	12.19	0.65
12	14.72	15.67	14.52	6.46	1.40
13	17.27	22.31	17.90	29.20	3.64
14	15.56	19.05	15.56	22.44	0.00
15	14.88	17.85	14.87	19.95	0.08
16	17.17	21.84	17.84	27.17	3.86
17	15.36	18.43	15.35	19.93	0.10
18	14.11	17.21	14.65	21.96	3.84
19	13.10	15.98	13.94	22.01	6.46
20	16.71	21.27	17.71	27.27	6.01
21	14.82	17.69	15.06	19.37	1.64
22	13.96	16.40	14.31	17.49	2.52
23	12.80	15.10	13.54	17.97	5.83
24	11.88	13.74	12.72	15.63	7.09
25	14.97	19.52	15.66	30.45	4.64
26	12.95	16.61	13.57	28.29	4.77
27	12.51	15.59	12.99	24.61	3.80
28	14.78	19.03	15.54	28.77	5.16
29	12.74	16.01	13.34	25.69	4.70
30	11.79	14.95	12.73	26.89	8.03
31	10.88	13.87	12.11	27.56	11.31
32	14.24	18.52	15.42	30.02	8.30
33	12.25	15.38	13.09	25.57	6.91
34	11.57	14.26	12.45	23.24	7.54
35	10.75	13.13	11.78	22.11	9.54
36	10.04	11.96	11.07	19.10	10.30
Average				21.72	4.14

the predicted residual strengths are for the A-basis yield strength. Results based on the B-basis yield strength are similar. If the results predicted by the models and the test values were identical, all of the points would fall on a diagonal line. The results from the modified LU model WSU2 are much closer to the diagonal line than are the results from the original LU model. Points below the diagonal line indicate that the model predicts conservative values, whereas points above that diagonal line indicate that the model overpredicts the test values. The results given in Tables 3 and 4 show that the average error increases with increasing nominal lead crack length. This was not the case in earlier investigations of the open-hole stiffened[4] and unstiffened[3] panels. In the earlier investigations, the antibuckling fixtures were placed directly over the crack line. However, for the bolted lap joint panels, the antibuckling fixtures were placed above and below the overlapped section, as shown in Fig. 2, which may allow more out-of-plane displacement, especially with the longer lead crack lengths.

The residual strengths of the panel configurations with a lead crack only (no MSD cracks) were used as references to investigate the effect of MSD on the panel's residual strength. Figure 5 shows the effect of MSD cracks on the residual strength of the panels, where the MSD crack length on the horizontal axis is plotted against the normalized residual strength (NRS) on the vertical axis. The NRS is the residual strength for a panel with an MSD crack divided by the residual strength of a panel with no MSD crack, with the lead crack length being the same. For example, the NRSs of panels 9–13 are obtained by dividing by their residual strengths by the residual strength for panel 8. The NRSs in Fig. 5 are based on the modified LU model predictions (for the A-basis yield strength) rather than the test values. The purpose of Fig. 5 is to show the reduction in residual strength based on MSD size. That is, Fig. 5 shows the increasing loss of strength with increasing MSD size. Table 5 contains the data used to plot the points in Fig. 5. A careful

Table 5 Normalized residual strength based on A-basis yield strengths

Panel	a, in.	e, in.	c, in.	σ_{WSU2}, ksi	NRS
1	4.19375	0.1	0	20.6	1
2	4.19375	0.1	0.05	17.91	0.869
3	4.19375	0.1	0.1	17.12	0.831
	4.19375	0.1	0.02	18.53	0.899
4	4.24375	0.15	0	20.54	1
5	4.24375	0.15	0.05	17.66	0.86
6	4.24375	0.15	0.1	16.83	0.819
7	4.24375	0.15	0.15	16.02	0.78
8	4.29375	0.2	0	20.36	1
9	4.29375	0.2	0.05	17.35	0.852
10	4.29375	0.2	0.1	16.45	0.808
11	4.29375	0.2	0.15	15.59	0.766
12	4.29375	0.2	0.2	14.68	0.721
13	5.19375	0.1	0	18	1
14	5.19375	0.1	0.05	15.66	0.87
15	5.19375	0.1	0.1	14.98	0.832
16	5.24375	0.15	0	17.95	1
17	5.24375	0.15	0.05	15.46	0.861
18	5.24375	0.15	0.1	14.77	0.822
19	5.24375	0.15	0.15	14.07	0.784
	5.24375	0.15	0.02	16.03	0.893
20	5.29375	0.2	0	17.84	1
21	5.29375	0.2	0.05	15.18	0.851
22	5.29375	0.2	0.1	14.44	0.809
23	5.29375	0.2	0.15	13.68	0.767
24	5.29375	0.2	0.2	12.87	0.721
25	6.19375	0.1	0	15.75	1
26	6.19375	0.1	0.05	13.66	0.867
27	6.19375	0.1	0.1	13.08	0.831
28	6.24375	0.15	0	15.64	1
29	6.24375	0.15	0.05	13.43	0.859
30	6.24375	0.15	0.1	12.84	0.821
31	6.24375	0.15	0.15	12.21	0.781
32	6.29375	0.2	0	15.54	1
33	6.29375	0.2	0.05	13.2	0.849
34	6.29375	0.2	0.1	12.56	0.808
35	6.29375	0.2	0.15	11.9	0.766
36	6.29375	0.2	0.2	11.2	0.721
	6.29375	0.2	0.02	13.75	0.885

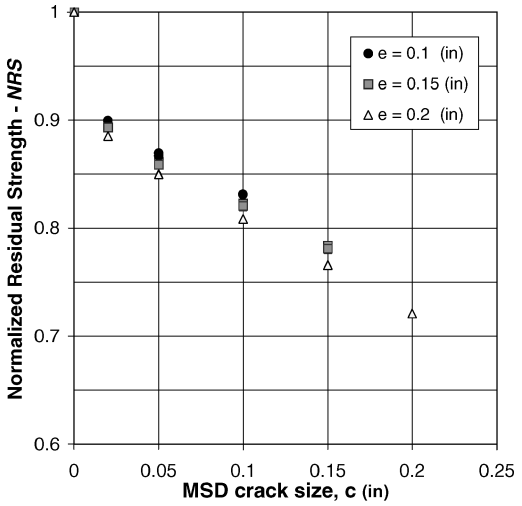

Fig. 5 Effect of MSD cracks size on residual strength.

examination of the data shows the NRS to be somewhat independent of the nominal lead crack length. For example, panels 3, 15, and 27 all have the same NRS. However, the NRS decreases slightly with increasing values of e. This is demonstrated with panels 3, 6, and 10, which have increasingly larger values of e and decreasingly smaller values of NRS. Table 5 contains three additional (unnumbered) panels, with a smaller MSD crack size ($c = 0.02$ in.), which are not included in Tables 1–4 because they were not tested. The residual strengths for these panels were determined from Eq. (2) for

A-basis yield strength. They were used to obtain additional points, arguably representing earlier stages of MSD cracks. The data in Fig. 5 show about 10% knockdown in residual strength at that early stage of MSD cracking ($c = 0.02$ in.), then the residual strength decreases linearly with increasing MSD cracks size.

Conclusions

A modified LU model previously developed by semi-empirical analysis of test data from 40 open-hole panels and validated with test data from 36 stiffened panels has been further examined. The residual strength predictions from the modified LU model correlated well with test data from 36 bolted lap joint panels. The modified LU model is significantly more accurate than the original LU model. It has been developed to be used with either A-basis or B-basis yield strength values. When compared with test data from the 36 panels with bolted joints, the modified model has an average error of 4.7% when used with A-basis yield strength and 4.1% when used with B-basis yield strength. The original LU model has average errors of 18.7% and 21.7% when used with A-basis and B-basis yield strengths, respectively. Although all of the 36 test panels had the same width, thickness, and hole pattern, each had a different crack configuration. The modified LU model shows a reduction in residual strength of approximately 10% at the early stages of MSD cracks and a nearly linear decrease of NRS as the MSD crack size increases.

The results of this study serve as an example of how a complex nonlinear problem can be represented by a rather simple semi-empirical model. It also demonstrates the idea that a stress intensity factor based model may be developed by empirical analysis with test data from a simple configuration, then be used to analyze more complex configurations, as long as the SIF for the more complex configurations can be determined.

Acknowledgments

This work was sponsored by the industrial members of the Aircraft Design and Manufacturing Research Center of Wichita State University, Wichita, Kansas. The material for the aluminum panels was donated by Alcoa Aerospace Center, Hutchinson, Kansas.

References

[1]Hijazi, A., "Residual Strength of Thin-Sheet Aluminum Panels with Multiple Site Damage," Ph.D. Dissertation, Dept. of Aerospace Engineering, Wichita State Univ., Wichita, KS, Dec. 2001.

[2]Swift, T., "Widespread Fatigue Damage Monitoring Issues and Concerns," *Proceedings of the 5th International Conference on Structural Airworthiness of New and Aging Aircraft*, Hamburg, Germany, June 1993.

[3]Smith, B., Saville, P., Mouak A., and Myose, R., "Strength of 2024-T3 Aluminum Panels with Multiple Site Damage," *Journal of Aircraft*, Vol. 37, No. 2, 2000, pp. 325–331.

[4]Smith, B., Hijazi, A., Haque, A. K. M., and Myose, R., "Strength of Stiffened Panels with Multiple Site Damage," *Journal of Aircraft*, Vol. 38, No. 4, 2001, pp. 764–768.

[5]Broek, D., "The Effects of Multi-Site Damage on the Arrest Capability of Aircraft Fuselage Structure," FractuResearch, TR 9302, Galena, OH, June 1993.

[6]Ingram, J. E., Kwon, Y. S., Duffie, K. J., and Irby, W. D., "Residual Strength Analysis of Skin Splices with Multiple Site Damage," *Proceedings of the Second Joint NASA/FAA/DoD Conference on Aging Aircraft*, edited by Charles E. Harris, 1999, pp. 427–436; also NASA CP-1999-208982.

[7]"Military HandBook of Metallic Materials and Elements for Aerospace Vehicles and Structures," MIL-HDBK-5G, Dept. of Defense, Nov. 1994.

[8]Dawicke, D. A., Newman, J. C., Jr., Sutton, M. A., and Amstutz, B. E., "Stable Tearing Behavior of a Thin Sheet Material with Multiple Cracks," NASA TM-109131, July 1994.

[9]Heinimann, M. B., "Analysis of Stiffened Panels with Multiple Site Damage," Ph.D. Dissertation, School of Aeronautics and Astronautics, Purdue Univ., West Lafayette, IN, May 1997.

[10]Secton, D. G., "A Comparison of Fatigue Damage Resistance and Residual Strength of 2024-T3 and 2524-T3 Panels Containing Multiple Site Damage," M.S. Thesis, School of Aeronautics and Astronautics, Purdue Univ., West Lafayette, IN, May 1997.

[11]James, M., and Swenson, D., "FRANC2D/L: A Crack Propagation Simulator for Plane Layered Structures," Kansas State Univ., Manhattan, KS, Available at URL: http://www.mne.ksu.edu/∼franc2d/.

[12]Cope, D., and Lacy, T., "Modeling Mechanical Fasteners in Lap Joints for Stress Intensity Determination," *Proceedings of the 4th Annual NASA/FAA/DoD Conference on Aging Aircraft*, May 2000; also Technical Paper AIAA/ASME/ASCE/AHS/ASC Structures, Structural Dynamics and Materials Conference, Vol. 1, No. 1, 2000, pp. 274–283.

[13]Swift, T., "Fracture Analysis of Stiffened Structures," Damage Tolerance of Metallic Structures: Analysis Methods and Application, American Society for Testing and Materials, ASTM STP 842, Los Angeles, CA, 1984, pp. 69–107.